Identification of KvLQT1 K^+ channels as new regulators of non-small cell lung cancer cell proliferation and migration

ALBAN GIRAULT[1,2], ANIK PRIVÉ[1], NGUYEN THU NGAN TRINH[1,2], OLIVIER BARDOU[1,2], PASQUALE FERRARO[1,3], PHILIPPE JOUBERT[4], RICHARD BERTRAND[1,2] and EMMANUELLE BROCHIERO[1,2]

[1]Centre de Recherche du Centre Hospitalier de l'Université de Montréal (CRCHUM), Montreal, Quebec H2X 0A9; Departments of [2]Medicine and [3]Surgery, University of Montreal, Montreal, Quebec H3C 3J7; [4]Centre de Recherche de l'IUCPQ, Quebec, Quebec G1V 4G5, Canada

Received October 24, 2013; Accepted November 25, 2013

DOI: 10.3892/ijo.2013.2228

Abstract. K^+ channels, which are overexpressed in several cancers, have been identified as regulators of cell proliferation and migration, key processes in cancer development/propagation. Their role in lung cancer has not been studied extensively; but we showed previously that KvLQT1 channels are involved in cell migration, proliferation and repair of normal lung epithelial cells. We now investigated the role of these channels in lung cancer cell lines and their expression levels in human lung adenocarcinoma (AD) tissues. First, we observed that the wound-healing rates of A549 lung adenocarcinoma cell monolayers were reduced by clofilium and chromanol or after silencing with KvLQT1-specific siRNA. Dose-dependent decrease of A549 cell growth and cell accumulation in G0/G1 phase were seen after KvLQT1 inhibition. Clofilium also affected 2D and 3D migration of A549 cells. Similarly, H460 cell growth, migration and wound healing were diminished by this drug. Because K^+ channel overexpression has been encountered in some cancers, we assessed KvLQT1 expression levels in tumor tissues from patients with lung AD. KvLQT1 protein expression in tumor samples was increased by 1.5- to 7-fold, compared to paired non-neoplastic tissues, in 17 of 26 patients. In summary, our data reveal that KvLQT1 channel blockade efficiently reduces A549 and H460 cell proliferation and migration. Moreover, KvLQT1 overexpression in AD samples suggests that it could be a potential therapeutic target in lung cancer.

Introduction

After injury, cell migration and proliferation are important mechanisms of tissue repair to restore airway and alveolar epithelia in several respiratory diseases (1-4). However, uncontrolled cell growth, dysregulation of cell motility and acquisition of an invasive phenotype are some of the hallmarks of cancer development and propagation (5,6). In fact, cell proliferation and motility are regulated by many actors, including growth factors and down-stream signalling effectors. However, a growing body of evidence demonstrates that K^+ channels also participate in the control of cell motility and growth of various cell types (7-13). Indeed, inhibiting or silencing of voltage-dependent (Kv), calcium-activated (KCa), inward-rectifying (Kir) and 2-pore (K2P) channels reduces the proliferation of numerous normal and cancer cells *in vitro* (14-22) and animal models (20,23,24). The mechanisms underlying the regulation of cellular proliferation by K^+ channels may be manifold, but evidence points to cell cycle control (10,25-27). In addition, K^+ channels could also be involved in tumor cell invasion and metastasis propagation via regulation of cell migration (11,14,28-31).

The role of K^+ channels in lung cancer has not been studied extensively. It has been shown that the inhibition of Girk channels (21) in small-cell lung cancer (SCLC) cells and Kv1.3 channels in non-small-cell lung cancer (NSCLC) A549 cells (20) has anti-proliferative effects. We previously reported the involvement of different types of K^+ channels, including a member of the Kv channel subfamily, KvLQT1, in the control of normal alveolar and bronchial epithelial cell proliferation, migration and epithelial repair (18,19). However, the participation of this channel in lung tumor cells has not been reported. Growing interest in K^+ channels as therapeutic targets in cancer is not only due to their role in cell growth and motility, but also because they have been found to be overexpressed in various tumor tissues, including in lung cancer (16,23,25,31-36). However, to the best of our knowledge, possible KvLQT1 overexpression in lung adenocarcinoma (AD) has never been observed.

In the present study, we first examined the mRNA expression of 3 Kv channels; KvLQT1, EAG1 and ERG1. The impact of pharmacological inhibition of these channels, with various drugs, was then evaluated in scratch assays. Because chromanol and clofilium reduced wound-healing rates more efficiently than astemizole and ergtoxin, we verified the involvement of KvLQT1 via a molecular approach with specific siRNA.

Correspondence to: Dr Emmanuelle Brochiero, Centre de Recherche du CHUM, Tour Viger, Room 08-424, 900 rue Saint-Denis, Montreal, QC H2X 0A9, Canada
E-mail: emmanuelle.brochiero@umontreal.ca

Key words: KvLQT1, K^+ channels, cell growth, motility, lung cancer

The impact of KvLQT1 inhibitors on A549 cell motility and proliferation mechanisms was then assessed. KvLQT1 was also investigated in wound healing, migration and growth of another lung cancer cell line: H460. Finally, KvLQT1 expression levels were measured in tumor tissues from patients with lung AD.

Materials and methods

Lung tissue samples. Our protocol on human tissues has been approved by the Ethics Committee of our Institution (Comité d'éthique à la recherche du CHUM). All participants provided their written informed consent to participate in this study and all clinical investigation has been conducted according to the principles expressed in the Declaration of Helsinki. Tumor and matched, adjacent, non-neoplastic lung tissues were sourced from 26 patients with lung adenocarcinoma (AD), the most common subtype of NSCLC. Tissues were collected immediately after surgical resection at the CHUM Hôpital Notre-Dame (Montréal, Québec, Canada) or obtained from the tissue bank of the Respiratory Health Network of the FRQS. Tissues were dissected from surgical samples by a pathologist, who confirmed the diagnosis of primary lung cancer and established clinical and histological parameters. The different growth patterns were quantified using a 5% increment by a thoracic pathologist, who classified the AD tumor samples based on the latest IASLC classification (37), into the following sub-categories: i) AD *in situ* (1 patient), ii) lepidic-predominant AD [4 patients, including formely non-mucinous bronchioloalveolar carcinoma (BAC) class], iii) acinar-predominant AD (8 patients), iv) papillary-predominant AD (3 patients), v) micropapillary-predominant AD (2 patients) and vi) solid-predominant AD (4 patients) as well as vii) invasive mucinous AD (4 patients, formely mucinous BAC). As reported in Table I, among the 26 patients included in our study, 46% were men and 54% were women, with a median age of 66 years (range 39-77 years); 76% had a smoking history. No patients in our cohort had metastasis at the time of lung resection.

Cell culture. A549 and H460 lung cancer cells were purchased from the ATCC and maintained in culture medium (A549: DMEM, Gibco, Invitrogen, Burlington, ON, Canada; H460: RPMI, Gibco, Invitrogen) supplemented with 10% of fetal bovine serum (FBS, Gibco, Invitrogen), 2 mM L-glutamine (Gibco, Invitrogen) and 50 U/ml penicillin and 50 μg/ml streptomycin (Gibco, Invitrogen).

Wound-healing assays. The commonly-employed 'wound-healing assay', which gives an estimation of the capacity of cells to migrate and proliferate (Fig. 1A) after mechanical injury, was used. Briefly, A549 and H460 cell monolayers were injured mechanically with a pipette tip (6 wounds/Petri dish), then washed to remove detached/injured cells, before photography with a Nikon camera under light microscopy (x4 enlargement). Marks on the Petri dishes allowed us to photograph the wounds exactly at the same place at various times, with measurement of the wound areas initially and after repair, by ImageJ software (National Institutes of Health), as described previously (38,39). The results, reported as the rates of wound closure in μm^2/h, are compared to the controls and in the presence of K^+ channel inhibitors, i.e., clofilium (Sigma-Aldrich, Oakville, ON, Canada), chromanol (Tocris, Bristol, UK), ergtoxin (Alomone Labs Ltd., Jerusalem, Israel) and astemizole (Tocris). Wound-healing rates were also evaluated in the presence of negative controls or KvLQT1 siRNAs (Invitrogen). For Ki67 staining during wound healing (Fig. 1A), confluent A549 cell monolayers, cultured on glass slides in Flexiperm (Dako Denmark, Glostrup, Denmark), were fixed in cold methanol at time 0 after injury and after 18 h of repair before staining with anti-Ki67 antibody (Dako), then Alexa Fluor 488 goat anti-mouse secondary antibody (proliferating cells stained in green) and finally counterstaining with DAPI (staining of nuclei in blue, Sigma).

Video-microscopy time-lapse experiments. The 2D cell migration rates (μm/h) of non-confluent A549 cells were evaluated by single-cell tracking with Axiovision software (Carl Zeiss, Toronto, ON, Canada) on sequence images captured at 5-min intervals over an 18-h period by digital camera connected to a Carl Zeiss microscope (Carl Zeiss, x10 enlargement).

Cell migration in Boyden-type chamber. The 3D migratory capacities of A549 and H460 cells were evaluated by Boyden-type chamber migration assay (18,19). Briefly, cells obtained after trypsinization were counted, and cell viability was verified by trypan blue assay. The cell suspensions were then placed in the upper compartment of 8-μm pore filters (0.33 cm^2, ThinCerts-TC inserts, Greiner Bio-one; MJS Biolynx, Brockville, ON, Canada) coated on the lower side with a collagen matrix. After cell migration, the filters were washed with PBS, and the cells were fixed with paraformaldehyde-acetone solution, then stained with hematoxylin. Non-migrating cells of the upper compartment were scrapped-off with cotton-tipped applicators (Fisher, Napean, ON, Canada), whereas migrating cells that passed through the lower face of the filters were counted in 5 different randomly-chosen fields by a light-inverted microscope at x20 magnification (18,19).

Cell proliferation and cell cycle analyses. A549 and H460 cell growth was evaluated by counting cell number over a 72-h period. Briefly, the cells were cultured at low density (15,000/cm^2) in 35-mm Petri dishes for 24 h in the absence of inhibitor. At this time (T0), they were exposed or not to K^+ channel inhibitors for 24-72 h, then separated with trypsin-EDTA (0.05%, Gibco, Invitrogen) at times 0, 24, 48 and 72 h, before counting by hemacytometer. The absence of drug cytotoxicity was verified by trypan-blue exclusion assay. At the end of growth assays, A549 cells were fixed in ethanol (70%) for cell cycle analysis. After centrifugation, they were re-suspended in PBS supplemented with pancreatic RNase A (Roche, Mannheim, Germany). After 30 min, propidium iodide solution (1 mg/ml, Sigma-Aldrich) was added to each sample, and flow cytometry performed with a flow Coulter EpicsXL cytometer (Beckman Coulter, Inc., Mississauga, ON, Canada). Data were recorded for at least 10,000 events, and signals were analyzed by Expo32 software (Applied Cytometry Systems, Sheffield, UK).

KvLQT1 channel silencing with siRNAs. As described previously (40), A549 cells (40-50% confluence) were exposed to control siRNAs (Stealth siRNA-negative control, 12935-400,

Table I. KvLQT1 expression ratio [in tumor vs non-tumor (non-neoplastic) tissue], with individual demographic and histopathological characteristics for the 26 patients included in the study.

Patient no.	Sex	Age	Smoking history	AD histological subtype	KvLQT1 ratio level (tumor/non-tumor)
1	F	62	No	AD *in situ*	2.0
2	M	67	No	Lepidic predominant (70%) and papillary (30%) patterns	5.0
3	M	43	Yes	Lepidic predominant (95%) and acinar (5%) patterns	0.3
4	F	66	Yes	Lepidic predominant (75%) and acinar (25%) patterns	1.1
5	F	71	No	Lepidic predominant (80%), acinar (10%) and papillary (10%) and papillary (10%) patterns	1.9
6	M	72	No	Acinar predominant (60%), micropapillary (30%) and lepidic (10%) patterns	1.4
7	F	77	Yes	Acinar predominant (55%) and lepidic (45%) patterns	1.3
8	F	77	No	Acinar predominant (40%), lepidic (20%), solid (20%) and papillary (10%) patterns	0.7
9	M	73	Yes	Acinar predominant (90%) and micropapillary (10%) patterns	1.7
10	M	59	Yes	Acinar predominant (75%), lepidic (20%) and solid (5%) patterns	2.8
11	F	71	Yes	Acinar predominant (80%) and papillary (20%) patterns	1.6
12	F	52	Yes	Acinar predominant (40%), micropapillary (30%), solid (20%) and papillary (10%) patterns	3.4
13	F	76	Yes	Acinar predominant (70%) and lepidic (30%) patterns	1.1
14	M	40	Yes	Papillary predominant (60%) and lepidic (40%) patterns	3.6
15	M	62	Yes	Papillary predominant (60%), lepidic (30%) and micropapillary (10%) patterns	4.5
16	M	39	?	Papillary predominant (80%), acinar (10%) and lepidic (10%) patterns	6.0
17	F	72	Yes	Micropapillary predominant (70%) and lepidic (30%) patterns	3.0
18	F	73	Yes	Micropapillary predominant (100%)	1.6
19	M	60	Yes	Solid predominant (90%) and acinar (10%) patterns and pleomorphic features	0.9
20	F	44	Yes	Solid predominant pattern (100%)	3.3
21	M	71	Yes	Solid (70%) predominant, micropapillary (20%) and acinar (10%) patterns	2.9
22	M	50	Yes	Solid predominant (70%) and acinar (30%) patterns with clear cells and cribriform (30%) features	2.4
23	F	66	No	Invasive mucinous AD	1.1
24	F	63	Yes	Invasive mucinous AD	1.5
25	F	74	Yes	Invasive mucinous AD	6.8
26	M	61	Yes	Invasive mucinous AD	0.5

AD, adenocarcinoma; KvLQT1 ratio, KvLQT1 protein expression in tumor tissue normalized to KvLQT1 expression in paired non-tumor tissue (from the same patient). Ratio >1.5 were considered as KvLQT1 overexpression.

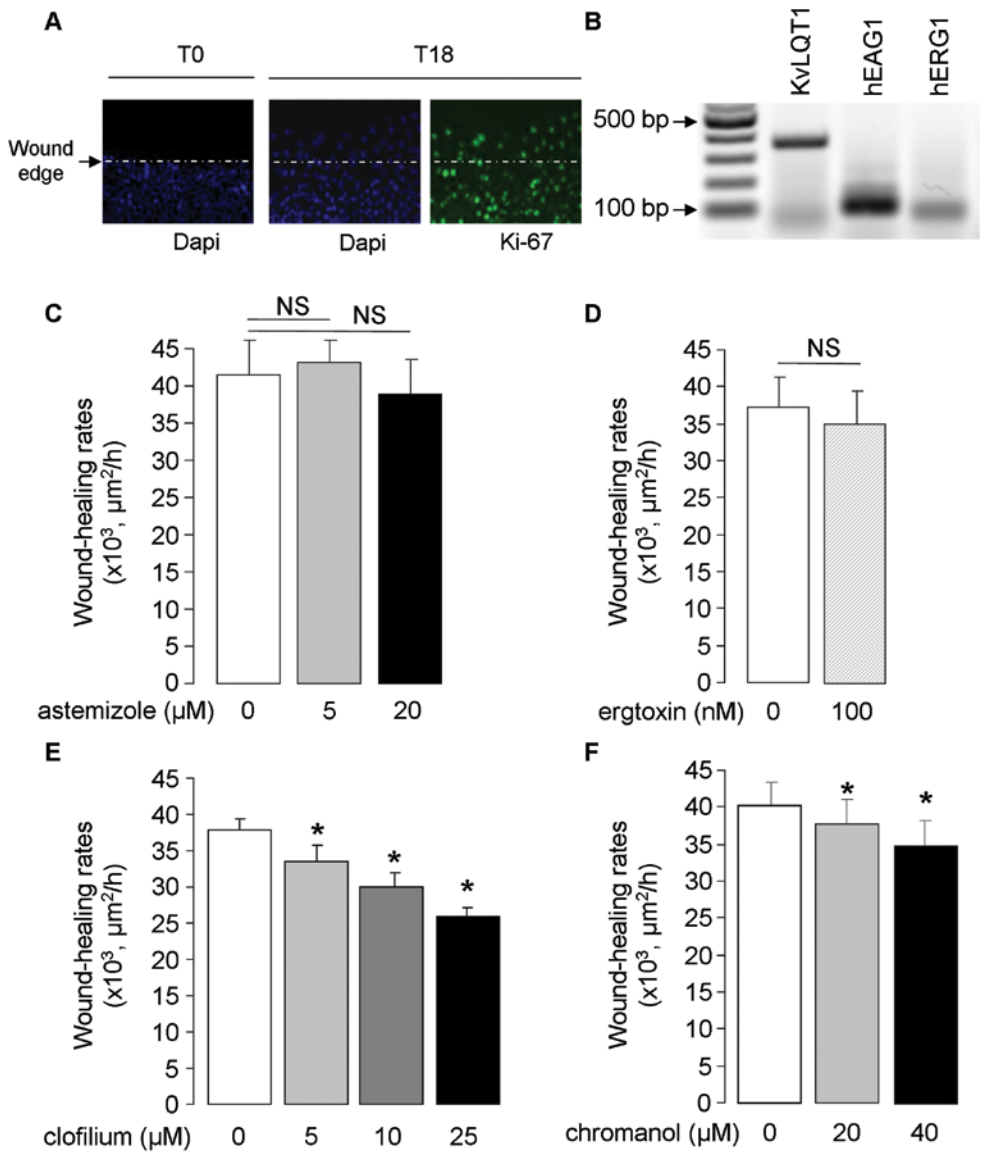

Figure 1. Detection of Kv K^+ channels and impact of their inhibition on wound healing in A549 cell monolayers. (A) Representative photograph (at x20 magnification) showing cell migration as well as active cell proliferation, indicated by Ki67 staining (green), at the wound edge of a repairing A549 cell monolayers. (B) Representative agarose gel showing PCR products amplified from A549 cell cDNA with PCR primer pairs designed from human KvLQT1, EAG1 and ERG1 K^+ channels. A549 cell monolayers were injured mechanically and wound healing was followed over an 18-h period. Wound-closure rates (μm^2/h) were compared in the control condition (0) and in the presence of astemizole [5 and 20 μM, n=5; (C)], ergtoxin [100 nM, n=5; (D)], clofilium [5, 10 or 25 μM, n=5; (E)] and chromanol [20 or 40 μM, n=8); (F)]. $^*p<0.05$.

100 pmol, Invitrogen) or siRNA directed against KvLQT1 (Stealth™ siRNA duplex oligonucleotides; Kcnq1-HSS142716, Invitrogen, 100 pmol), mixed with Lipofectamine™ RNAiMax transfection reagent in OptiMEM (Invitrogen). Fresh, complete DMEM was added onto cells after 5-h exposure to siRNAs, and then replaced every 24 h for 72-96 h. Transfection efficiency >90% was observed under these experimental conditions (40).

Reverse transcription-polymerase chain reaction (RT-PCR) amplification. Total RNA purified from A549 cells with TRIzol reagent (Invitrogen) was reverse-transcribed with MMLV reverse transcriptase (Invitrogen) in the presence of oligodT primers. cDNAs were amplified with Taq polymerase (Invitrogen), and specific primers designed from sequences of human KvLQT1 [Kv7.1 (41), NM_000218, 5'-taaggaagagccc aacactg-3', 5'-cgatccttgctcttttctga-3', 1 μM, 355-bp product], human ether-a-go-go 1 (hEAG1, Kv10.1, NM_002238.3, 5'-gag aacgtggatgagggcat-3', 5'-gtagtggtccagcttacggg-3', 1 μM, 96-bp product), human ether-a-go-go-related gene (hERG1, Kv11.1, NM_000238.3, NM_172056.2, 5'-ggccagagccgtaagttcat-3', 5'-aagccgtcgttgcagtagat-3', 1 μM, 74-bp product) and β-actin (hβ-actin, 5'-agagctacgagctgcctgac-3', 5'-aaagccatgccaatctcatc-3', 0.25 μM, 499-bp product), for normalization. Primer pairs were designed in distinct exons to avoid genomic DNA amplification. KvLQT1, EAG and ERG products were amplified for 30 cycles, while β-actin amplification was stopped after 18 cycles. RT-PCR products were finally separated on 1% agarose gel and stained with SYBR® Safe (Invitrogen). Signals were detected by Typhoon Gel Imager and analyzed by ImageQuant software (Molecular Dynamics, Baie d'Urfe, QC, Canada). KvLQT1 silencing with siRNA was also verified by RT-PCR (40).

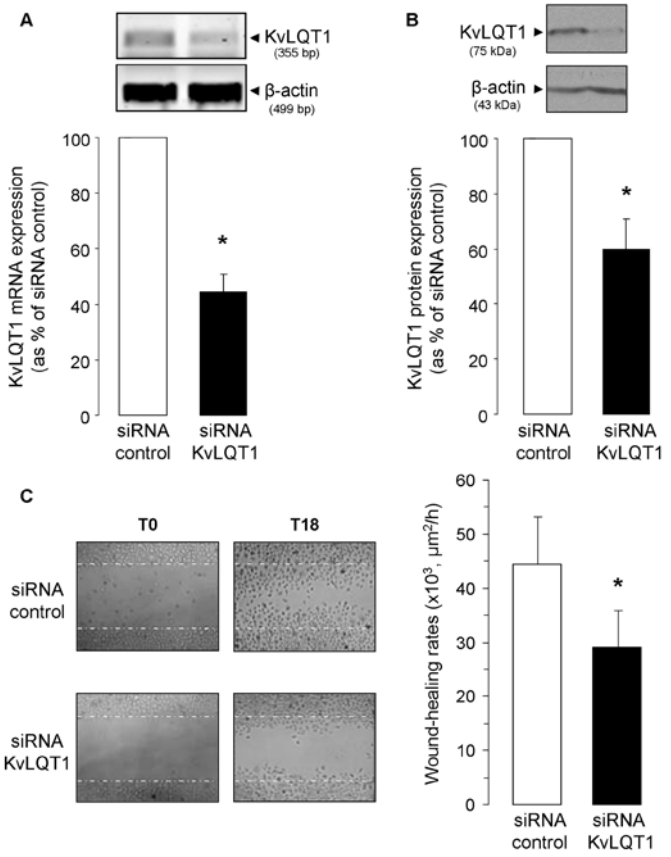

Figure 2. Delayed wound healing in A549 cell monolayers after KvLQT1 silencing. A549 cells (at 40-50% confluency) were transfected with negative control siRNA (siRNA control) or KvLQT1 siRNA in the presence of RNAiMax. KvLQT1 silencing was verified by PCR [(A), n=10] and western blotting with KvLQT1 antibody [(B), n=7]. (C) Wound-healing rates (in μm^2/h) were measured at 18 h after injury among cells transfected with negative control siRNA or KvLQT1 siRNA (n=9). Representative photographs (x4 magnification) at 0 and 18 h are presented (left panel). The white lines represent the initial wound edge. *p<0.05.

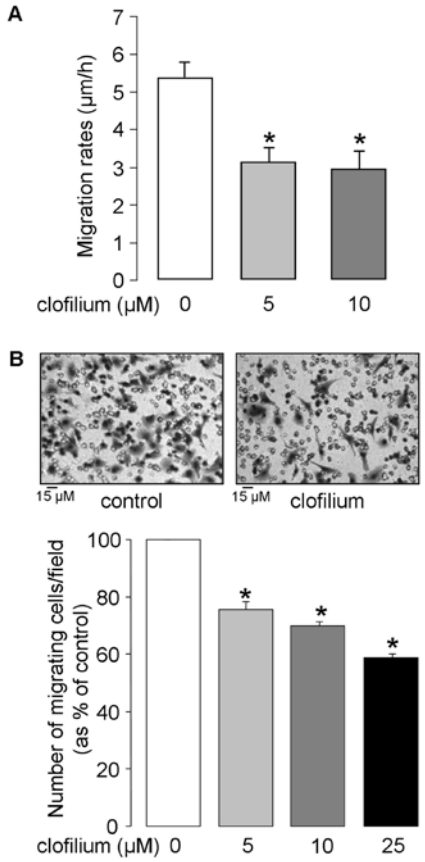

Figure 3. Involvement of KvLQT1 in 2D and 3D A549 cell migration. (A) 2D cell migration rates (μm/h) were evaluated by A549 single-cell tracking (~30 cells/field, 2 fields/condition/experiment, n=3) in live time-lapse video-microscopy over an 18-h period in the absence (0) or presence of clofilium (5 or 10 μM). (B) The number of migrating A549 cells was measured over an 18-h period in a Boyden-type chamber (3D migration) in the absence (0) or presence of 5, 10 or 25 μM clofilium in both the lower and upper compartments (5 fields/insert, 3 inserts/condition, n=5). Representative photographs (x20 magnification) of the lower side of the inserts showing hematoxylin stained migrating cells in control and clofilium (25 μM) conditions appears above. *p<0.05.

Immunoblotting. Immunoblotting was undertaken according to a well-established laboratory protocol (18,40). Total A549 proteins were solubilized in lysis buffer [150 mM NaCl, 50 mM Tris-HCl, pH 7.6, 1% Triton X-100, 0.1% SDS, protease inhibitor cocktail (Complete Mini EDTA-free protease inhibitor cocktail, Roche)] on ice for 30 min. Proteins from lung tissues were extracted by homogenization, with a glass putter for 2 min in lysis buffer (150 mM NaCl, 25 mM Tris-HCl, 1 mM EDTA, leupeptin, aprotinin, PMSF protease and orthovanadate phosphatase inhibitors). Cell lysates were centrifuged, supernatants collected, and protein concentration measured by Bradford assay. Proteins were separated by SDS-PAGE and transferred onto nitrocellulose membranes. After blocking, the membranes were incubated with anti-KvLQT1 (sc-10645, Santa Cruz Biotechnology, Inc., Santa Cruz, CA, USA) and anti-β-actin antibodies (CLT9001, Cedarlane Laboratory Ltd., Burlington, ON, Canada) on the same blot, to ensure equivalent loading. KvLQT1 antibody specificity was verified with its blocking peptide [sc10645P, Santa Cruz, (18)]. After washing, the membranes were incubated with donkey anti-goat (for KvLQT1, Santa Cruz Biotechnology, Inc.) and horse anti-mouse (for β-actin; Cell Signaling Technology, Boston, MA, USA) IgG linked to horseradish peroxidase for 1 h. The intensity of each specific band was quantified with ChemiDoc XRS+ Molecular Imager and Image Lab software (Bio-Rad, Mississauga, ON, Canada), then normalized to the β-actin signal.

Statistical analyses. The data are presented as mean ± standard error of the mean (SEM) and were compared with Statview software (SAS Institute, Cary, NC, USA). Statistical analyses were made using paired Student's t-test, Wilcoxon signed rank test and one sample sign test. For comparison between more than two means, we used Friedman analysis followed by Dunn's test. Differences were considered significant when $p<0.05$.

Results

Detection of Kv channels and impact of their inhibition on wound healing in A549 cell monolayers. The presence of human KvLQT1, EAG1 and ERG1 mRNA was first detected by RT-PCR in lung AD A549 cells (Fig. 1B). To evaluate the

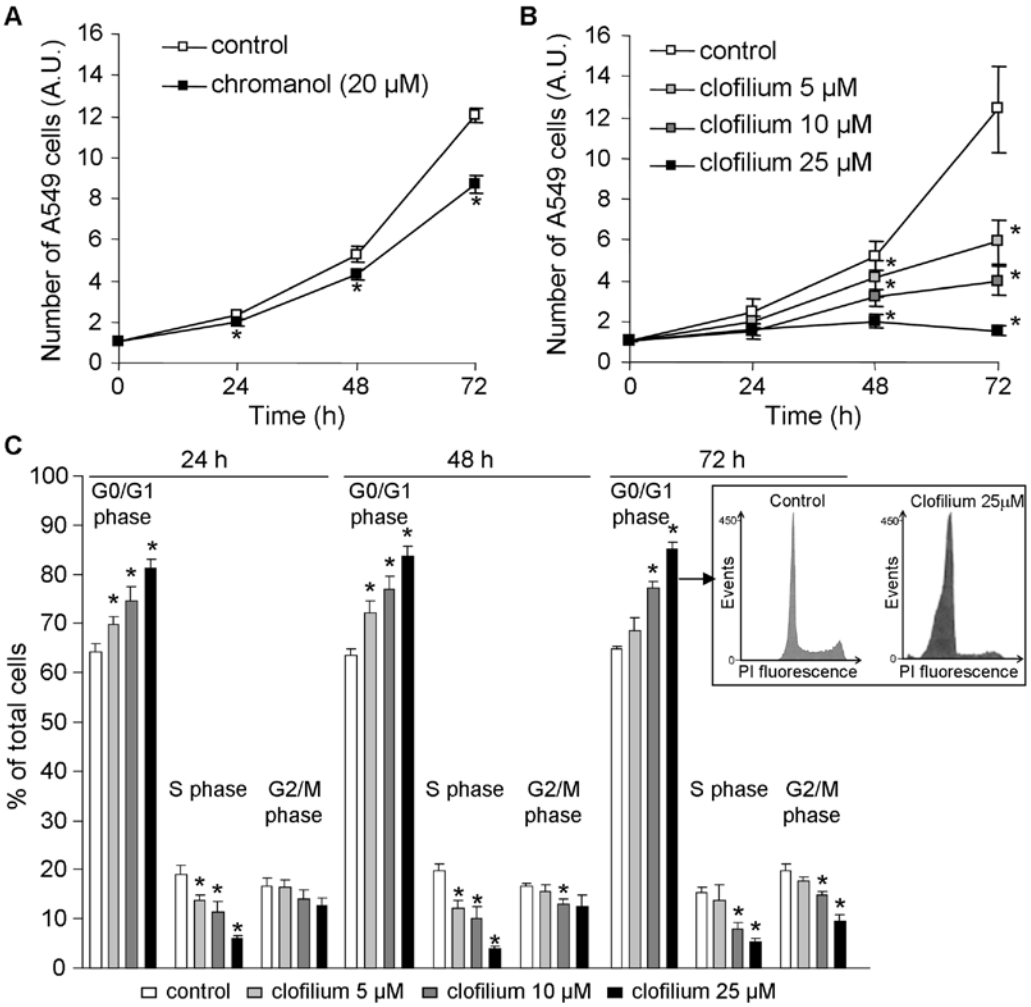

Figure 4. Impact of KvLQT1 inhibition on proliferation and cell cycle distribution. Sub-confluent A549 cells were incubated with chromanol [20 μM, n=6; (A)] and increasing clofilium concentrations [5, 10 or 25 μM, n=7; (B)] for 24, 48 or 72 h. Cell growth was then estimated at each time-point by counting the number of A549 cells after cell separation by trypsinization. Values are reported in arbitrary units, normalized to the number of cells at time 0. $^*p<0.05$. (C) Cell cycle distribution of A549 cells, after 24-, 48- or 72-h exposure to 5, 10 or 25 μM clofilium was assessed by analyzing isolated nuclei stained with propidium iodide by flow cytometry. Bar diagrams show the percentages of cells in the G0/G1, S and G2/M phases. The results are expressed as mean percentage of total cells ± SEM of 5-7 experiments. $^*p<0.05$. Insert, flow cytometry histograms of A549 cells in the control condition and after 72-h treatment with 25 μM clofilium.

contribution of these channels, A549 cells were exposed to various pharmacological Kv channel inhibitors in scratch-assays, which engages cell migration and proliferation processes (Fig. 1A). Neither astemizole (EAG and ERG channel inhibitor, 5 and 20 μM), nor ergtoxin (specifically blocking ERG channels, 100 nM) significantly affected A549 wound-healing rates (Fig. 1C and D). On the contrary, clofilium, which is frequently used to study KvLQT1 function in respiratory epithelia (42-44), dose-dependently decreased wound-healing rates of A549 cell monolayers (11, 21 and 31% inhibition in the presence of 5, 10 and 25 μM clofilium, respectively, Fig. 1E). Similarly, the KvLQT1 blocker chromanol reduced A549 wound healing (Fig. 1F).

To confirm the role of KvLQT1, we adopted a complementary approach with stealth KvLQT1 siRNAs to test if its specific silencing would subsequently affect wound-healing rates. First, the efficiency of KvLQT1 siRNA in downregulating KvLQT1 mRNA (Fig. 2A) and protein (Fig. 2B) expression was verified. We then found that partial KvLQT1 silencing elicited a significant decrease in wound-healing ($28.9\pm6.9\times10^3$ μm^2/h, Fig. 2C), compared to A549 cells exposed to negative control siRNA ($44.3\pm8.9\times10^3$ μm^2/h, i.e., 35% inhibition). Data from both pharmacological and molecular approaches thus point toward KvLQT1 involvement in the regulation of A549 wound healing. We then undertook complementary assays to dissect its implication in both cell migration and proliferation.

Impact of clofilium on A549 cell motility. The effect of clofilium on 2D cell migration dynamics was assessed by single-cell tracking of sub-confluent A549 cells in time-lapse video-microscopy experiments. As illustrated in Fig. 3A, cell migration rates were reduced by 42% in the presence of 5 μM clofilium; no further inhibition (45%) was elicited by higher (10 μM) clofilium concentration. 3D cell motility, an important determinant of cancer propagation, was then estimated by Boyden-type chamber assay. It was observed that the number of cells migrating through the chambers was significantly reduced by clofilium (25, 31 and 42% inhibition at 5, 10 and

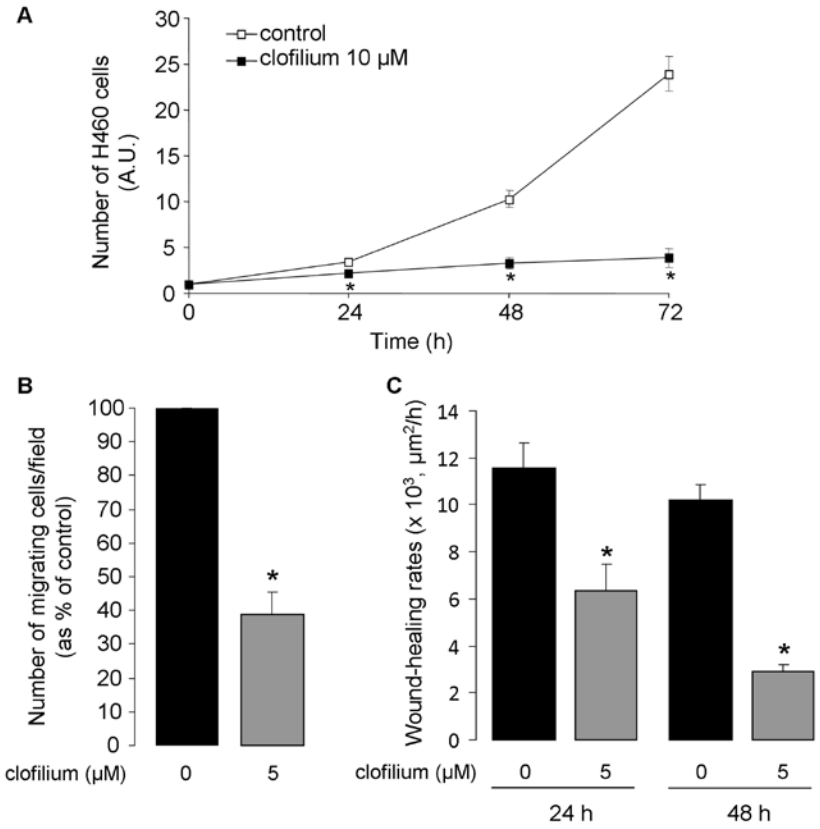

Figure 5. Impact of KvLQT1 inhibition on H460 cell proliferation, migration and wound-healing rates. (A) H460 cells were incubated with clofilium (10 μM) for 24, 48 or 72 h. Cell growth was then estimated at each time-point by counting the number of H460 cells after cell separation by trypsinization. Values are reported in arbitrary units, normalized to the number of cells at time 0 (n=6). (B) The number of migrating H460 cells was measured over a 24-h period in a Boyden-type chamber in the absence (0) or presence of 5 μM clofilium (5 fields/insert, 3 inserts/condition, n=9). (C) H460 cell monolayers were injured mechanically, and wound healing was followed over a 24- to 48-h period. Wound-closure rates (μm^2/h) were compared in the control condition (0) and in the presence of 5 μM clofilium (n=8). *p<0.05.

25 μM, respectively, Fig. 3B). Altogether, these data indicate that clofilium could depress 2D and 3D A549 cell motility.

Anti-proliferative effect of KvLQT1 inhibition through A549 cell cycle control. Because cell proliferation is a crucial component of tumor growth, we then evaluated KvLQT1's contribution to cell proliferation, by counting the number of A549 cells after a 24- to 72-h period in the presence of KvLQT1 inhibitors. We noted that 20 μM chromanol significantly reduced cell growth, compared to untreated cells (Fig. 4A). Similarly, increasing clofilium concentrations (from 5 to 25 μM) decreased A549 cell proliferation in a dose- and time-dependent manner (Fig. 4B). At the 72-h post-treatment time-point, we estimated that <5 μM of clofilium was required to inhibit 50% of cell growth.

It has been proposed that cell cycle control by K^+ channels may be a possible mechanism whereby they could regulate cell proliferation (10,25-27,45). We thus decided to examine the effect of 24-, 48- and 72-h clofilium application on A549 cell cycle distribution, by flow cytometry. First, it has to be mentioned that clofilium, even at 25 μM concentration for 72 h, did not elicit cytotoxicity as indicated by the absence of significant accumulation of sub-G0 apoptotic cells (Fig. 4C, insert). Moreover, we discerned a dose-dependent effect of clofilium on the cell cycle with an increasing number of cells in the G0/G1 phase and subsequent reduction of cells in the S and G2/M phases (Fig. 4C). These results showed that KvLQT1 inhibition in A549 cells significantly curbed cell proliferation and impacted cell cycle progression.

Reduction of H460 cell proliferation, migration and wound healing by clofilium. The effect of clofilium was also assessed in a second lung cancer cell model, the H460 cell line. As depicted in Fig. 5, KvLQT1 inhibition severely reduced H460 cell growth (Fig. 5A) and migration in the Boyden-type chamber (Fig. 5B). Accordingly, healing rates, measured at 24 and 48 h after wounding, were affected by clofilium (Fig. 5C).

KvLQT1 protein overexpression in tumor tissues from patients with lung AD. KvLQT1 expression levels were then examined by immunoblotting of human lung AD tumor tissues, compared to matched, adjacent, non-neoplastic lung parenchyma, from 26 patients (Fig. 6 and Table I). An elevation (1.5- to 7-fold) of KvLQT1 protein was apparent in AD tumor tissues from 17 among 26 patients studied (i.e., 65%). More precisely, KvLQT1 overexpression (>1.5-fold) was found in 1/1 patient with AD *in situ*, 3/4 patients with lepidic-predominant AD, 4/8 patients with acinar-predominant AD, 3/3 patients with papillary-predominant AD, 1/2 patients with micropapillary-predominant AD, 2/4 patient with solid-predominant AD and 3/4 patients with invasive mucinous AD. KvLQT1 overexpres-

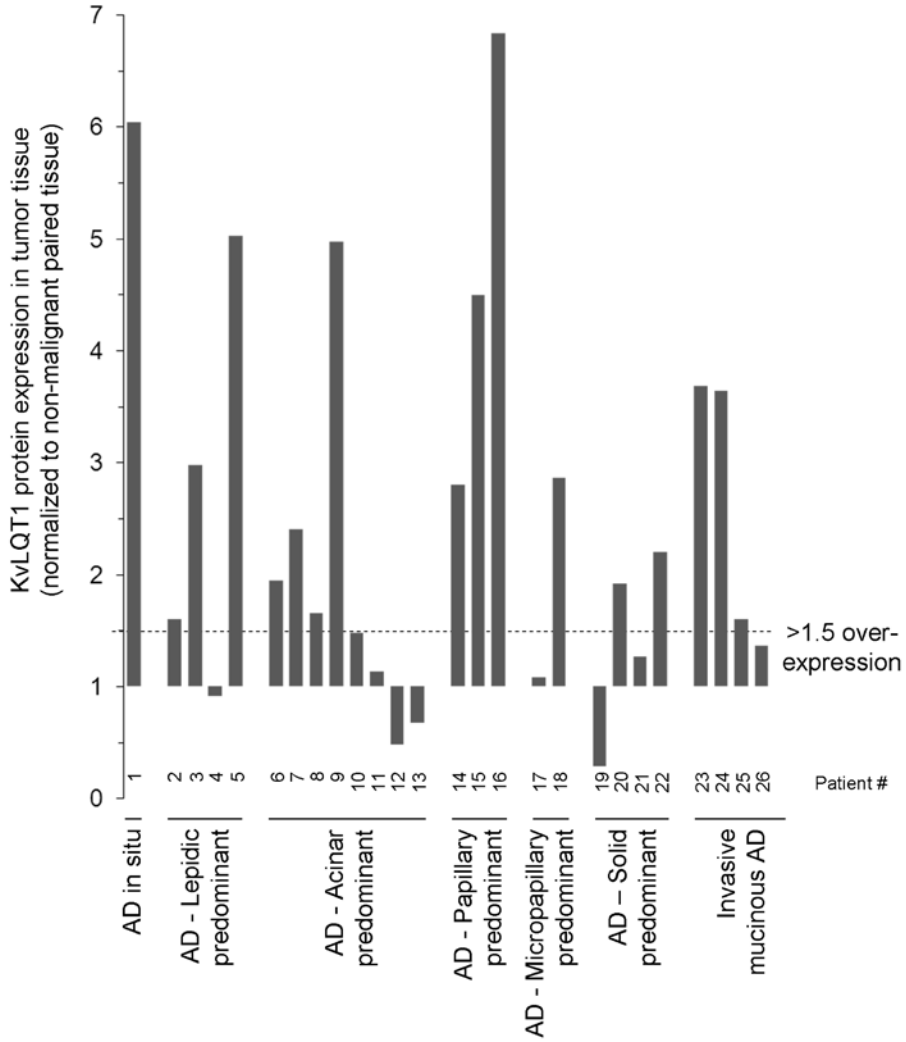

Figure 6. KvLQT1 overexpression in tumor tissues from patients with lung AD. KvLQT1 protein expression was evaluated by immunoblotting of proteins extracted from tumor and matched adjacent non-neoplastic tissues from 26 patients with different sub-types of lung AD. The results are presented for each patient as the ratio of KvLQT1 expression in tumor vs non-malignant tissues. Patients were separated into 7 groups: 1, AD *in situ* (patient no. 1); 2, lepidic- (patients no. 2-5); 3, acinar- (patients no. 6-13); 4, papillary- (patients no. 14-16); 5, micropapillary (patients nos. 17 and 18); 6, solid-predominant AD (patients no. 19-22) and 7, invasive mucinous AD (patients no. 23-26).

sion was detected in both males and females, with or without smoking history (Table I).

Discussion

Our data first disclosed that clofilium and chromanol as well as KvLQT1 silencing with siRNA significantly reduced the wound-healing rates of A549 monolayers. Moreover, A549 cell migration, proliferation and cell cycle were affected after KvLQT1 inhibition. The role of this channel was also verified in the lung cancer cell line H460. Finally, KvLQT1 overexpression was detected in 17 of 26 lung AD human samples.

KvLQT1, EAG1 and ERG1 mRNA was noted in A549 cells. However, application of ergtoxin failed to decrease A549 wound-healing rates. Similarly, astemizole, which blocks EAG and ERG channels, did not significantly affect wound healing, whereas clofilium, used frequently to study KvLQT1 channel function in respiratory epithelia (42-44), dose-dependently reduced wound healing. We are aware that this compound may have off-target effects, e.g., on TASK (46), EAG (47) and ERG (48) K^+ channels. However, higher clofilium concentrations (~100 μM) are necessary for TASK inhibition (46,49). Moreover, the absence of inhibitory effects of ergtoxin and astemizole suggests that the suppressive action of clofilium in our assays is mainly occurring via KvLQT1 inhibition. This hypothesis is reinforced by the observed inhibition of wound healing by chromanol and confirmed by data obtained after KvLQT1 silencing, which caused a marked decline of wound-healing rates.

The decrease in A549 and H460 cell growth with clofilium and/or chromanol that we report here is the first evidence of such a role for KvLQT1 in NSCLC cells. These results are in agreement with other studies showing that K^+ channel function modulates cell proliferation both *in vitro* and *in vivo* (9,10,15,16,23). In A549 cells, an anti-proliferative effect after Kv1.3 inhibition or silencing has already been cited (20). In SCLC cells, the involvement of other K^+ channels in proliferation, i.e., Girk (21) and 4-AP sensitive K^+ channels (22), has been demonstrated.

Our results indicate that KvLQT1 may regulate cell growth by controlling cell cycle progression from the G0/G1 to the S phase. Indeed, clofilium blockade affected cell cycle distribution, with a dose-dependent increase of A549 cells in the G0/G1 phase (and a decrease in G2/M and S). A similar result was observed after Kv1.3 silencing in the same cell model (20). The regulation of cell proliferation by K^+ channels, through cell cycle control, has also been postulated in many other cancer types (10,45,50). Moreover, it has been hypothesized that transient hyperpolarization, after K^+ channel activation, could be essential for G1 phase progression (10,50,51). In fact, other mechanisms, including calcium signaling, changes in cell volume and/or activation of signaling pathways, e.g., may also be involved (10,15,20,27,50).

Our experiments provide proof that clofilium not only decreases cell proliferation but also 2D and 3D cell migration, as shown by time-lapse video-microscopy and Boyden-type chamber assays. This is the first evidence of KvLQT1 involvement in lung cancer cell motility/proliferation, although we previously described its role in non-cancer alveolar and bronchial cells (18,19). Our present study is in agreement with previous reports that the migration of other cancer cells is reduced by inhibiting or silencing many K^+ channel types (11,14,29-31). Several hypotheses have been proposed to explain how these channels regulate cell migration, e.g., through the modulation of membrane potential, cell volume, intracellular calcium and signaling pathways (11). However, it has also been proposed that K^+ channels may regulate cell motility through their coupling with migratory machinery proteins, such as integrins (52).

At present, it is not clear if KvLQT1 protein *per se* or its K^+ conducting function is responsible for the observed effect of KvLQT1 modulation on cell migration/proliferation. However, the inhibitory effect of clofilium and/or chromanol indicates that K^+ conductance via KvLQT1 may be involved. Similarly, K^+ permeation is the central mechanism by which TASK3 exerts its oncogenic potential *in vitro* and *in vivo*, as supported by experiments on point mutations at the channel pore (53). In contrast, another study showed that ERG protein downregulation after silencing reduced SCLC cell proliferation, whereas its blockade had no impact, suggesting that its ion-conducting property was unnecessary (54).

Our western blot analysis of tissues from patients with lung AD revealed, for the first time, KvLQT1 overexpression ranging from 1.5- to 7-fold, in 17/26 of them. To the best of our knowledge, our study provides the first evidence of KvLQT1 overexpression in lung cancer tissues, although higher KvLQT1 protein levels have already been reported in testicular seminoma tumor samples (35) and in gastrointestinal cancers (36). Other K^+ channels (Girk, TASK3) have also been shown to be overexpressed in SCLC tissues (21,32). In fact, higher expression levels of many K^+ channels have been detected in several cancer tissue types (16,23,31-36), and it has been demonstrated that their overexpression highly increased cell proliferation/migration (14,15). It is not yet clear why K^+ channels are modulated in cancer tissues but it has been postulated that they may be regulated during cell dedifferentiation or by high cytokine levels found in tumors (25).

Elevated KvLQT1 levels were detected in our study in all AD tested sub-categories, including AD *in situ*, lepidic-, acinar-, papillary-, micropapillary-, solid-predominant AD as well as invasive mucinous AD. However, a larger cohort would be necessary to define if the frequency and level of KvLQT1 overexpression change among these different classes. Moreover, patient number was not sufficient to establish a possible correlation between KvLQT1 expression level and cancer severity (e.g., tumor grade or the presence of lymph node metastasis). Nevertheless, correlation between clinical parameters and prognosis outcomes with K^+ channel expression has already been reported in other studies (reviewed in ref. 12).

In conclusion, our data demonstrate for the first time, efficient reduction of A549 and H460 cell growth/motility after KvLQT1 inhibition, with clofilium and/or chromanol. Our study highlights increased expression of this channel in human AD samples. It would thus be interesting to further evaluate KvLQT1's oncogenic potential promise and the potential effect of KvLQT1 inhibitors on lung cancer development *in vivo*.

Acknowledgements

We thank Dr P. Romeo, pathologist at the CHUM and the tissue bank of the FRQS Respiratory Health Network, for providing human tissue samples. We acknowledge the logistical assistance received from the Research Support Office, CRCHUM. This study was funded by the Canadian Institutes of Health Research (CIHR, MOP-111054), the CRCHUM and Université de Montréal (scholarship to E.B.), the CIHR training program of the Respiratory Health Network and the Fonds de Recherche du Québec - Santé (fellowships to A.G.).

References

1. Berthiaume Y, Lesur O and Dagenais A: Treatment of adult respiratory distress syndrome: plea for rescue therapy of the alveolar epithelium. Thorax 54: 150-160, 1999.
2. Sacco O, Silvestri M, Sabatini F, Sale R, Defilippi AC and Rossi GA: Epithelial cells and fibroblasts: structural repair and remodelling in the airways. Paediatr Respir Rev 5 (Suppl A): S35-S40, 2004.
3. Zahm JM, Kaplan H, Herard AL, Doriot F, Pierrot D, Somelette P and Puchelle E: Cell migration and proliferation during the in vitro wound repair of the respiratory epithelium. Cell Motil Cytoskeleton 37: 33-43, 1997.
4. Crosby LM and Waters CM: Epithelial repair mechanisms in the lung. Am J Physiol Lung Cell Mol Physiol 298: L715-L731, 2010.
5. Hanahan D and Weinberg RA: Hallmarks of cancer: the next generation. Cell 144: 646-674, 2011.
6. Mareel M and Leroy A: Clinical, cellular, and molecular aspects of cancer invasion. Physiol Rev 83: 337-376, 2003.
7. Prevarskaya N, Skryma R and Shuba Y: Ion channels and the hallmarks of cancer. Trends Mol Med 16: 107-121, 2010.
8. O'Grady SM and Lee SY: Molecular diversity and function of voltage-gated (Kv) potassium channels in epithelial cells. Int J Biochem Cell Biol 37: 1578-1594, 2005.
9. Wonderlin WF and Strobl JS: Potassium channels, proliferation and G1 progression. J Membr Biol 154: 91-107, 1996.
10. Villalonga N, Ferreres JC, Argiles JM, Condom E and Felipe A: Potassium channels are a new target field in anticancer drug design. Recent Pat Anticancer Drug Discov 2: 212-223, 2007.
11. Schwab A, Hanley P, Fabian A and Stock C: Potassium channels keep mobile cells on the go. Physiology 23: 212-220, 2008.
12. Arcangeli A, Crociani O, Lastraioli E, Masi A, Pillozzi S and Becchetti A: Targeting ion channels in cancer: a novel frontier in antineoplastic therapy. Curr Med Chem 16: 66-93, 2009.

13. Girault A, Haelters JP, Potier-Cartereau M, Chantome A, Jaffres PA, Bougnoux P, Joulin V and Vandier C: Targeting SKCa channels in cancer: potential new therapeutic approaches. Curr Med Chem 19: 697-713, 2012.
14. Afrasiabi E, Hietamaki M, Viitanen T, Sukumaran P, Bergelin N and Tornquist K: Expression and significance of HERG (KCNH2) potassium channels in the regulation of MDA-MB-435S melanoma cell proliferation and migration. Cell Signal 22: 57-64, 2010.
15. Huang L, Li B, Li W, Guo H and Zou F: ATP-sensitive potassium channels control glioma cells proliferation by regulating ERK activity. Carcinogenesis 30: 737-744, 2009.
16. Lallet-Daher H, Roudbaraki M, Bavencoffe A, Mariot P, Gackiere F, Bidaux G, Urbain R, Gosset P, Delcourt P, Fleurisse L, Slomianny C, Dewailly E, Mauroy B, Bonnal JL, Skryma R and Prevarskaya N: Intermediate-conductance Ca^{2+}-activated K^+ channels (IKCa1) regulate human prostate cancer cell proliferation through a close control of calcium entry. Oncogene 28: 1792-1806, 2009.
17. Alvarez-Baron CP, Jonsson P, Thomas C, Dryer SE and Williams C: The two-pore domain potassium channel KCNK5: induction by estrogen receptor alpha and role in proliferation of breast cancer cells. Mol Endocrinol 25: 1326-1336, 2011.
18. Trinh NT, Prive A, Kheir L, Bourret JC, Hijazi T, Amraei MG, Noel J and Brochiero E: Involvement of KATP and KvLQT1 K^+ channels in EGF-stimulated alveolar epithelial cell repair processes. Am J Physiol Lung Cell Mol Physiol 293: L870-L882, 2007.
19. Trinh NT, Prive A, Maille E, Noel J and Brochiero E: EGF and K^+ channel activity control normal and cystic fibrosis bronchial epithelia repair. Am J Physiol Lung Cell Mol Physiol 295: L866-L880, 2008.
20. Jang SH, Choi SY, Ryu PD and Lee SY: Anti-proliferative effect of Kv1.3 blockers in A549 human lung adenocarcinoma in vitro and in vivo. Eur J Pharmacol 651: 26-32, 2011.
21. Plummer HK, III, Dhar MS, Cekanova M and Schuller HM: Expression of G-protein inwardly rectifying potassium channels (GIRKs) in lung cancer cell lines. BMC Cancer 5: 104, 2005.
22. Pancrazio JJ, Tabbara IA and Kim YI: Voltage-activated K^+ conductance and cell proliferation in small-cell lung cancer. Anticancer Res 13: 1231-1234, 1993.
23. Wang ZH, Shen B, Yao HL, Jia YC, Ren J, Feng YJ and Wang YZ: Blockage of intermediate-conductance-Ca(2+) -activated K(+) channels inhibits progression of human endometrial cancer. Oncogene 26: 5107-5114, 2007.
24. Gomez-Varela D, Zwick-Wallasch E, Knotgen H, Sanchez A, Hettmann T, Ossipov D, Weseloh R, Contreras-Jurado C, Rothe M, Stuhmer W and Pardo LA: Monoclonal antibody blockade of the human Eag1 potassium channel function exerts antitumor activity. Cancer Res 67: 7343-7349, 2007.
25. Felipe A, Vicente R, Villalonga N, Roura-Ferrer M, Martinez-Marmol R, Sole L, Ferreres JC and Condom E: Potassium channels: new targets in cancer therapy. Cancer Detect Prev 30: 375-385, 2006.
26. Woodfork KA, Wonderlin WF, Peterson VA and Strobl JS: Inhibition of ATP-sensitive potassium channels causes reversible cell-cycle arrest of human breast cancer cells in tissue culture. J Cell Physiol 162: 163-171, 1995.
27. Zhanping W, Xiaoyu P, Na C, Shenglan W and Bo W: Voltage-gated K^+ channels are associated with cell proliferation and cell cycle of ovarian cancer cell. Gynecol Oncol 104: 455-460, 2007.
28. Restrepo-Angulo I, Sanchez-Torres C and Camacho J: Human EAG1 potassium channels in the epithelial-to-mesenchymal transition in lung cancer cells. Anticancer Res 31: 1265-1270, 2011.
29. Hammadi M, Chopin V, Matifat F, Dhennin-Duthille I, Chasseraud M, Sevestre H and Ouadid-Ahidouch H: Human ether a-gogo K(+) channel 1 (hEag1) regulates MDA-MB-231 breast cancer cell migration through Orai1-dependent calcium entry. J Cell Physiol 227: 3837-3846, 2012.
30. Yasukagawa T, Niwa Y, Simizu S and Umezawa K: Suppression of cellular invasion by glybenclamide through inhibited secretion of platelet-derived growth factor in ovarian clear cell carcinoma ES-2 cells. FEBS Lett 586: 1504-1509, 2012.
31. Potier M, Joulin V, Roger S, Besson P, Jourdan ML, Leguennec JY, Bougnoux P and Vandier C: Identification of SK3 channel as a new mediator of breast cancer cell migration. Mol Cancer Ther 5: 2946-2953, 2006.
32. Mu D, Chen L, Zhang X, See LH, Koch CM, Yen C, Tong JJ, Spiegel L, Nguyen KC, Servoss A, Peng Y, Pei L, Marks JR, Lowe S, Hoey T, Jan LY, McCombie WR, Wigler MH and Powers S: Genomic amplification and oncogenic properties of the KCNK9 potassium channel gene. Cancer Cell 3: 297-302, 2003.
33. Ohya S, Kimura K, Niwa S, Ohno A, Kojima Y, Sasaki S, Kohri K and Imaizumi Y: Malignancy grade-dependent expression of k(+)-channel subtypes in human prostate cancer. J Pharmacol Sci 109: 148-151, 2009.
34. Voloshyna I, Besana A, Castillo M, Matos T, Weinstein IB, Mansukhani M, Robinson RB, Cordon-Cardo C and Feinmark SJ: TREK-1 is a novel molecular target in prostate cancer. Cancer Res 68: 1197-1203, 2008.
35. Tsevi I, Vicente R, Grande M, Lopez-Iglesias C, Figueras A, Capella G, Condom E and Felipe A: KCNQ1/KCNE1 channels during germ-cell differentiation in the rat: expression associated with testis pathologies. J Cell Physiol 202: 400-410, 2005.
36. Than BL, Goos JA, Sarver AL, O'Sullivan MG, Rod A, Starr TK, Fijneman RJ, Meijer GA, Zhao L, Zhang Y, Largaespada DA, Scott PM and Cormier RT: The role of KCNQ1 in mouse and human gastrointestinal cancers. Oncogene: Aug 26, 2013 (Epub ahead of print). doi: 10.1038/onc.2013.350.
37. Travis WD, Brambilla E, Noguchi M, Nicholson AG, Geisinger KR, Yatabe Y, Beer DG, Powell CA, Riely GJ, Van Schil PE, Garg K, Austin JH, Asamura H, Rusch VW, Hirsch FR, Scagliotti G, Mitsudomi T, Huber RM, Ishikawa Y, Jett J, Sanchez-Cespedes M, Sculier JP, Takahashi T, Tsuboi M, Vansteenkiste J, Wistuba I, Yang PC, Aberle D, Brambilla C, Flieder D, Franklin W, Gazdar A, Gould M, Hasleton P, Henderson D, Johnson B, Johnson D, Kerr K, Kuriyama K, Lee JS, Miller VA, Petersen I, Roggli V, Rosell R, Saijo N, Thunnissen E, Tsao M and Yankelewitz D: International association for the study of lung cancer/american thoracic society/european respiratory society international multidisciplinary classification of lung adenocarcinoma. J Thorac Oncol 6: 244-285, 2011.
38. Maille E, Trinh NT, Prive A, Bilodeau C, Bissonnette E, Grandvaux N and Brochiero E: Regulation of normal and cystic fibrosis airway epithelial repair processes by TNF-alpha after injury. Am J Physiol Lung Cell Mol Physiol 301: L945-L955, 2011.
39. Trinh NT, Bardou O, Prive A, Maille E, Adam D, Lingée S, Ferraro P, Desrosiers M, Coraux C and Brochiero E: Improvement of defective cystic fibrosis airway epithelial wound repair after CFTR rescue. Eur Respir J 40: 1390-1400, 2012.
40. Bardou O, Prive A, Migneault F, Roy-Camille K, Dagenais A, Berthiaume Y and Brochiero E: K(+) channels regulate ENaC expression via changes in promoter activity and control fluid clearance in alveolar epithelial cells. Biochim Biophys Acta 1818: 1682-1690, 2012.
41. Wang Q, Curran ME, Splawski I, Burn TC, Millholland JM, VanRaay TJ, Shen J, Timothy KW, Vincent GM, de Jager T, Schwartz PJ, Toubin JA, Moss AJ, Atkinson DL, Landes GM, Connors TD and Keating MT: Positional cloning of a novel potassium channel gene: KVLQT1 mutations cause cardiac arrhythmias. Nat Genet 12: 17-23, 1996.
42. Cowley EA and Linsdell P: Characterization of basolateral K^+ channels underlying anion secretion in the human airway cell line Calu-3. J Physiol 538: 747-757, 2002.
43. Devor DC, Bridges RJ and Pilewski JM: Pharmacological modulation of ion transport across wild-type and DeltaF508 CFTR-expressing human bronchial epithelia. Am J Physiol Cell Physiol 279: C461-C479, 2000.
44. MacVinish LJ, Hickman ME, Mufti DA, Durrington HJ and Cuthbert AW: Importance of basolateral K^+ conductance in maintaining Cl- secretion in murine nasal and colonic epithelia. J Physiol 510: 237-247, 1998.
45. Ouadid-Ahidouch H and Ahidouch A: K(+) channels and cell cycle progression in tumor cells. Front Physiol 4: 220, 2013.
46. Inglis SK, Brown SG, Constable MJ, McTavish N, Olver RE and Wilson SM: A Ba^{2+}-resistant, acid-sensitive K^+ conductance in Na^+-absorbing H441 human airway epithelial cells. Am J Physiol Lung Cell Mol Physiol 292: L1304-L1312, 2007.
47. Asher V, Warren A, Shaw R, Sowter H, Bali A and Khan R: The role of Eag and HERG channels in cell proliferation and apoptotic cell death in SK-OV-3 ovarian cancer cell line. Cancer Cell Int 11: 6, 2011.

48. Perry M, Stansfeld PJ, Leaney J, Wood C, de Groot MJ, Leishman D, Sutcliffe MJ and Mitcheson JS: Drug binding interactions in the inner cavity of HERG channels: molecular insights from structure-activity relationships of clofilium and ibutilide analogs. Mol Pharmacol 69: 509-519, 2006.
49. Niemeyer MI, Cid LP, Barros LF and Sepulveda FV: Modulation of the two-pore domain acid-sensitive K^+ channel TASK-2 (KCNK5) by changes in cell volume. J Biol Chem 276: 43166-43174, 2001.
50. Pardo LA: Voltage-gated potassium channels in cell proliferation. Physiology 19: 285-292, 2004.
51. Klimatcheva E and Wonderlin WF: An ATP-sensitive K(+) current that regulates progression through early G1 phase of the cell cycle in MCF-7 human breast cancer cells. J Membr Biol 171: 35-46, 1999.
52. Arcangeli A and Becchetti A: Complex functional interaction between integrin receptors and ion channels. Trends Cell Biol 16: 631-639, 2006.
53. Pei L, Wiser O, Slavin A, Mu D, Powers S, Jan LY and Hoey T: Oncogenic potential of TASK3 (Kcnk9) depends on K^+ channel function. Proc Natl Acad Sci USA 100: 7803-7807, 2003.
54. Glassmeier G, Hempel K, Wulfsen I, Bauer CK, Schumacher U and Schwarz JR: Inhibition of HERG1 K^+ channel protein expression decreases cell proliferation of human small cell lung cancer cells. Pflugers Arch 463: 365-376, 2012.